SYNTHESIS OF CHITOSAN-*GRAFT*-POLY(ETHYLENE GLYCOL) WITH THE ANTIBACTERIAL PROPERTY

Chau Ngoc Mai[1,2,3], La Thi Thai Ha[2,3,*], Tran Trung Hieu[2,3], Nguyen Thuy An[2,3]

[1]*Ho Chi Minh City University of Food Industry*

[2]*Ho Chi Minh City University of Technology*

[3]*Vietnam National University Ho Chi Minh City*

*Email: *lathaihapolyme@hcmut.edu.vn*

Received: 10 June 2022; Accepted: 25 July 2022

ABSTRACT

Chitosan (CS) is one of the most plenteous polymers in nature and itself has enormous potential due to its inherent antibacterial ability and exceptional properties as a biopolymer. However, its brittleness and low mechanical properties limited its utilization. Herein, poly(ethylene glycol) (PEG) was chosen to graft with CS to compensate for CS drawbacks owing to its high flexibility and safety to humans. This paper aimed at synthesizing CS graft PEG through a two-stage approach with high grafting efficiency and evaluating its antibacterial activity after modification. At first, PEG was conversed to PEG-aldehyde as an intermediate for the grafting copolymerization onto CS. The results showed that the $AgNO_3$ concentration of 0.75 wt % at the temperature of 80 °C was the optimum condition to obtain the highest conversion efficiency of ~ 77%. In the next stage, the grafting copolymerization was conducted by the reaction between $–NH_2$ groups in CS and –CHO groups in PEG–aldehyde. With the $–NH_2$/–CHO molar ratio of 10 and the $NaBH_4$/PEG-aldehyde molar ratio of 7.4, the grafting percentage and efficiency achieved the highest values (90 and 35%, respectively) after a 6-hour reaction. The CS–PEG could reduce the glass transition temperature of CS to – 31 °C, indirectly demonstrating the flexible enhancement of CS molecules while the antibacterial effect of CS–PEG reached 99.8 and 98.3% against *E. coli* and *S. aureus*, proving the high potential to be applied in the food industry as an antibacterial coating.

Keywords: Antibacterial polyme, chitosan *graft* poly(ethylene glycol), grafting copolymer, nature polymer.

1. INTRODUCTION

Chitosan (CS) has gained much attention globally as one of the well-known materials after cellulose owing to its non-toxicity, biocompatibility, biodegradability, anti-bacteria [1], and environmental friendliness [2] as a result of glycoside groups. In addition, CS originated from crustaceans, therefore low-price, plentiful, and always renewable in nature [2]. CS itself can withstand the growth of bacteria by adhering to the cells of negatively charged bacteria, thereby destroying the cells and permeating through the bacterial membrane to prevent DNA replication and gradually kill them [3]. However, several major weaknesses of CS have limited its applications in practice, such as high brittleness, low mechanical properties, and highly selective solubility in many solvents that need to be enhanced. Many attempts have been made to tailor the properties of CS by grafting copolymerization with other potential polymers

including grafting with *n*-butyl acrylate to reduce the brittle level and increase the flexibility [4], grafting with poly(*L*-lactide) to upgrade the biocompatibility and biodegradation for biomedical applications [5], grafting with poly(vinyl alcohol) to increase the tensile strength and elongation at break [6], or more recently grafting with polyaniline to obtain a conductive material [7]. Besides the majority of polymers mentioned above, poly(ethylene glycol) (PEG) is one of the most potential derivative choices to resolve the polymer chain brittleness of CS due to its high ductility, flexibility, and exceptional friendliness to human beings, enabling it to be applied in human-related fields such as cosmetic [2], tissue engineering and biotechnologies [8], and food preservative as an antimicrobial coating [9].

In this study, CS was grafted with PEG (CS–PEG) to reduce the general glass transition temperature of CS-based product and enhance the flexibility of the CS chains, thereby improving the mechanical and thermal properties. Moreover, the antibacterial effect of CS–PEG was also examined compared to the virgin CS, demonstrating that CS–PEG is a potential candidate to be applied in the medical and food industry sectors.

2. MATERIALS AND METHODOLOGY

2.1. Materials

Chitosan (CS) (M_w = 9155 g/mol with the deacetylation degree of ~ 70%) was kindly supplied from Chitosan VN (Vietnam). poly(ethylene glycol) (PEG) with M_w = 4155 g/mol was purchased in Vietnam. $AgNO_3$ and $NaBH_4$ (Merck, Germany), diethyl ether (Et_2O) (Chemsol, China), chloroform (ChL) (Chemsol, China), and acid acetic (AA) (China) were used as received.

2.2. Methodology

To graft PEG chains onto CS macromolecule, the aldehyde groups need to be generated first to become intermediate groups by oxidizing the alcohol groups of PEG with $AgNO_3$ and releasing silver nanoparticles (AgNPs) [10], facilitating the grafting process at the next stage.

2.2.1. Stage 1: Synthesis of PEG-aldehyde (PEG–CHO)

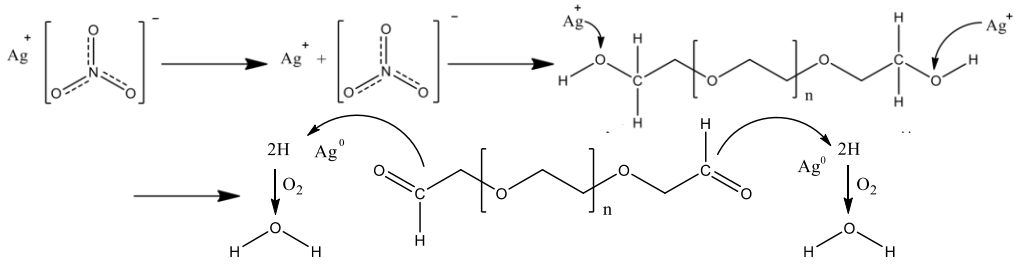

Figure 1. Reaction mechanism of PEG–CHO oxidated by $AgNO_3$.

First, 10 g of PEG solution 50 wt % in ChL was introduced into the bottom-rounded flask at the certain testing temperature (varied from 60 to 90 °C). Next, a $AgNO_3$ solution was added dropwise into the solution with a pre-determined concentration (ranging from 0.5 to 1.5 wt %) for 3 hours. The obtained yellowish-brown solution was diluted in ChL at a ratio of 1:4 (w/w). After being extracted to eliminate water and created AgNPs, the PEG-aldehyde product was

dissolved in Et_2O and then crystallized at 5 °C and was vacuum dried at room temperature prior to grafting copolymerization.

2.2.2. Stage 2: Synthesis of CS–PEG

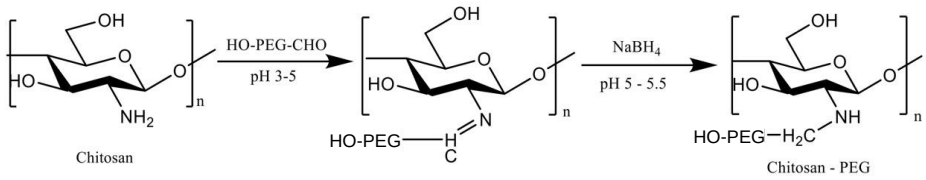

Figure 2. General reaction scheme of CS–PEG

50 g of CS solution 0.75% in AA was added into a 250 mL bottom-rounded flask. PEG-CHO with different amine/aldehyde molar ratios ($–NH_2$/–CHO = 20, 10, 5, and 2.5) was dissolved into AA solution 1% (with the mass ratio of PEG–CHO/AA = 1/4). The PEG–CHO solution was then introduced into the flask for 30 min at room temperature while the pH of the solution was adjusted from 3 to 5 with HCl solution 1 N. After 1-hour reaction, $NaBH_4$ solution 1.0% (with molar ratio of $NaBH_4$/PEG–CHO = 7.4) was added into the mixture and adjusted the pH of 5 – 5.5 with Na_2CO_3 solution to conduct the reduction reaction at 60 °C for 5 hours. The obtained CS–PEG product was vacuum dried at 90 °C for the solvent evaporation before further characterizations.

2.2.3. Characterizations

After the first stage, the PEG–CHO conversion efficiency (*RE %)* is calculated by the equation (1):

$$RE\,\% = \frac{m_{practical\ PEG-CHO}}{m_{theorical\ PEG-CHO}} \times 100 \qquad (1)$$

Soxhlet extraction was used to evaluate the the grafting percentage (*P %*) and grafting efficiency (*E %*) through the equations (2) and (3) below [4, 11]:

$$P\,\% = \frac{m_{CS-PEG} - m_{CS}}{m_{CS}} \times 100 \quad (2)\ ;\ E\,\% = \frac{m_{CS-PEG} - m_{CS}}{m_{PEG}} \times 100 \quad (3)$$

in which $m_{CS–PEG}$ is the mass of finally obtained product CS–PEG after removing all the remaining reagents through Soxhlet method; m_{PEG} and m_{CS} are the mass of PEG and CS respectively before grafting process. Fourier-transform infrared spectroscopy (FTIR) was obtained via TENSOR 27-BRUKER (Germany) to confirm the chemical structures of the virgin CS, PEG, PEG-aldehyde, and CS–PEG. The Ultraviolet-visible (UV-Vis) spectrum was used to evaluate the formation of AgNPs and conversion rate of aldehyde groups in the oxidation reaction through UV-2450 SHIMADZU Spectrophotometer in the wavelength range of 200 to 600 nm. The molecular weights of CS, PEG, and PEG–CHO were measured by Gel Permeation Chromatography (Cirrus GPC version 3.0) with the dilute solution of chloroform. Differential scanning calorimetry (DSC) method was utilized to determine the glass transition temperature of samples after the grafting reaction with the heating rate of 10 °C min^{-1}, under a nitrogen atmosphere from – 60 to 300 °C and carried out two cycles. The appearance and morphology of AgNPs was evaluated by Transmission electron microscopy (TEM, Jeol – Japan JEM 1400). The antibacterial properties of CS and CS–PEG were thoroughly tested with *S. aureus* ATCC 25923 in Baird Parker and *E. coli* ATCC 25922 in EMB (concentration of ~ 10^{-3} CFU mL^{-1}), exposure time of 1 hour by IP HCM V04:2017 method in Institut Pasteur in Ho Chi Minh City.

3. RESULTS AND DISCUSSION

3.1. Stage 1: Effects of temperature and $AgNO_3$ concentration on the formation of PEG–CHO and AgNPs

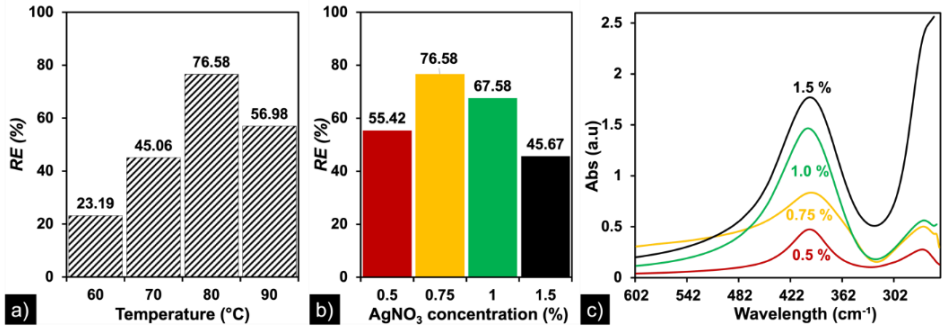

Figure 3. Effects of the temperature and the $AgNO_3$ concentration on the formation of PEG–CHO and AgNPs. a) Effect of reaction temperature; b) Effect of $AgNO_3$ concentration; c) UV-Vis curves of generated AgNPs in PEG–CHO solutions when the $AgNO_3$ concentration varied from 0.5 to 1.5%.

As can be seen in Figure 3a, with a similar $AgNO_3$ concentration of 0.75%, an increase in reaction temperature from 60 – 80 °C of the oxidation reaction creating PEG–CHO led to a rise in reaction efficiency (*RE %*), reaching the highest value of 76.58%. However, after exceeding 80 °C, the *RE %* decreased significantly to ~ 57% at 90 °C. This can be explained because the generated AgNPs from the oxidation-reduction reaction become more flexible and tend to aggregate at temperatures over 80 °C. The aggregate phenomenon, therefore, increases the average particle size of AgNPs and hinders the reactive groups of the aldehyde conversion reaction, leading to a decrease in *RE %* [12].

On the other hand, besides the reaction temperature, $AgNO_3$ concentration is also a crucial parameter in not only facilitating oxidation-reduction reaction but also determining the amount of generated AgNPs. In Figure 3b, at the fixed temperature of 80 °C, the *RE %* grows remarkably from 55.42% to 76.58%, corresponding to the $AgNO_3$ concentration increased from 0.5% to 0.75%. However, a sharp downward trend was witnessed when the $AgNO_3$ concentration is higher than 0.75%, dropping to 45.67% at the $AgNO_3$ concentration of 1.5 %. Literally, the more $AgNO_3$ concentration, the more AgNPs can be formed, causing a similar phenomenon of increasing reaction temperature. Figure 3c is presented to validate the amount of generated AgNPs by UV-Vis curves with a typical peak of 380 – 420 cm^{-1}. The morphology of AgNPs can be observed in TEM micrographs, verifying the nano-sized silver particles generated from the oxidation-reduction reaction of PEG and $AgNO_3$ (Figure 4).

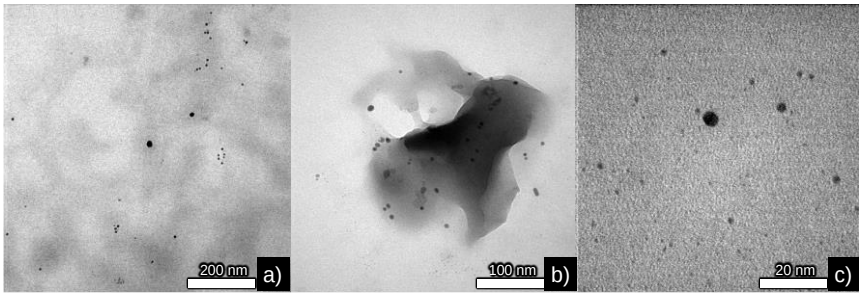

Figure 4. TEM micrographs of AgNPs generated in the oxidation-reduction reaction

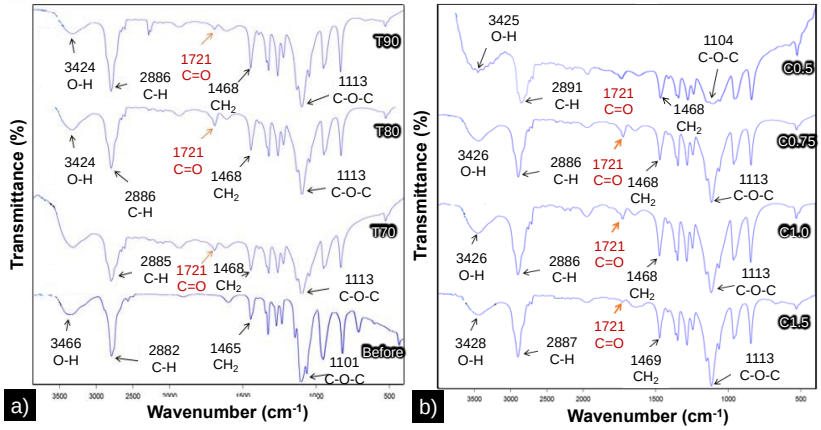

Figure 5. FTIR spectra demonstrating the effects of reaction temperature and $AgNO_3$ concentration on the obtained PEG–CHO structure. a) PEG before and after being conversed to PEG–CHO at 70, 80 and 90 °C, abbreviated as Before, T70, T80, and T90, respectively. b) PEG–CHO synthesized with different $AgNO_3$ concentration: 0.5, 0.75, 1.0, and 1.5%, entitled C0.5, C0.75, C1.0, and C1.5, respectively.

The differences in chemical structure of PEG-CHO after the conversion reaction with various conditions can be clearly seen through FTIR spectrum in Figure 5. Before the aldehyde conversion, PEG exhibits the typical vibration peaks, including the broad absorption peak at 3644 cm^{-1} of O–H stretching, 2882 cm^{-1} of C–H stretching, 1465 cm^{-1} of $–CH_2$ in aliphatic compounds, and C–O–C asymmetric stretching at 1101 cm^{-1}. After the conversion to PEG–CHO, a new peak appears at 1721 cm^{-1}, attributed to the C=O stretching vibration of the new –CHO groups. Moreover, compared to the methylene on the backbone at 1468 cm^{-1} which remained unchanged during the reaction, the peak intensity of T80 is relatively higher that of T70 and T90 (Figure 5a). Meanwhile, in Figure 5b, the $AgNO_3$ concentration over 0.75% may lead to a reduction in C=O peak intensity, meaning that the lower PEG–CHO was formed. This result once again confirmed the trend of *RE %* and the aforementioned statements that the sufficiently high $AgNO_3$ concentration and temperature lead to a hindrance in PEG–CHO synthetic reaction. At the end of this conversion reaction, the molecular weight of PEG–CHO stayed almost unchanged (M_w = 4081) compared to that of original PEG (M_w = 4155).

3.2. Stage 2: An effect of $–NH_2$/–CHO molar ratio on the grafting efficiency and grafting percentage of CS–PEG

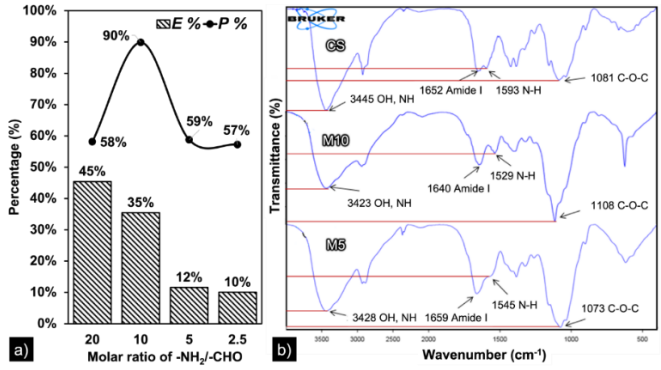

Figure 6. Effect of $–NH_2$/–CHO molar ratio on the grafting efficiency (*E %*) and grafting percentage (*P %*) (a) with corresponding chemical structures of the ratios of 10 and 5 shown in (b) (abbreviated as M10 and M5).

At the next stage, PEG is grafted onto the CS molecules through –CHO groups (as illustrated in Figure 2). Therefore, the molar ratio between $–NH_2$ groups in CS molecules and –CHO groups in PEG–CHO mainly determines the grafting efficiency (*E %*) and grafting percentage (*P %*) of this reaction. Note that, *E %* indicates the weight of grafted PEG versus the weight of the original PEG, while *P %* is the weight of grafted PEG compared to the original CS. In this study, the amount of CS was fixed while PEG–CHO was increasingly added to vary the $–NH_2$/–CHO ratios with other factors fixed. The results in Figure 6a indicate that the $–NH_2$/–CHO ratio is directly proportional to the *E %*, meaning that the larger amount of PEG–CHO causes the *E %* reduction. In other words, the grafted PEG insignificantly increases compared to the addition of a larger PEG–CHO amount (the denominator grows much faster than the numerator in the equation (3)). Meanwhile, the *P %* sharply rises from 58 to 90% when this ratio decreases from 20 to 10. This can be explained that at the ratio of 20/1, the PEG–CHO amount is much lower than CS; therefore, the –CHO groups are not sufficient to combine with all $–NH_2$ groups in CS, causing the small amount of grafted PEG. With the ratio of 10/1, an increased amount of PEG–CHO leads to a rise in the reacted $–NH_2$ groups in CS, thereby obtaining a higher grafted PEG and enlarging *P %* to 90%. After this ratio was lower than 10, the *P %* dropped dramatically to 59% due to the high viscosity of the general mixture and the steric hindrance of $–NH_2$ groups in CS, which reduces its reactivity. Moreover, the CS–PEG films cannot be formed with the molar ratios of 2.5 and 5.0 because of an excessive amount of PEG–CHO. The $–NH_2$/–CHO molar ratio of 10/1 resulted in the highest values of both *E %* and *P %* with the $NaBH_4$/PEG–CHO molar ratio of 7.4 and reaction time of 6 hours.

3.3. Chemical structure, thermal and antibacterial properties of CS–PEG

The typical chemical structures of CS–PEG and virgin CS can be observed in Figure 6b. The characteristic peaks of original CS fully appear in the FTIR spectra such as O–H and N–H stretching at 3445 cm^{-1}, amide I at 1652 cm^{-1}, N–H bending at 1593 cm^{-1}, and C–O–C vibration at 1081 cm^{-1}. After the grafting copolymerization through $–NH_2$ and –CHO groups, a separated and clearer peak of N–H moves to 1529 cm^{-1} due to a formation of amine II, along .with a far more intense peak of C–O–C stretching at ~ 1100 cm^{-1} compared to the O–H and N–H peak at ~ 3400 cm^{-1} of CS as a result of adding many PEG chains [13, 14]. This is a demonstration of successfully grafting PEG onto CS molecules. To further confirm, DSC measurement was utilized to examine the change in glass transition temperature (T_g) of CS (Figure 7). CS is highly brittle with the typical T_g of ~ 150 °C [15] whereas PEG is a flexible semicrystalline polymer with the T_g of – 50 °C [16,17]. The DSC result shows that T_g of CS–PEG is – 31.09 °C, proving an enormous enhancement in the flexibility of the copolymer after adding flexible PEG chains onto CS molecules. The next two endothermal peaks at 53.41 °C and 134.62 °C are assigned to the humid evaporation and dehydration of CS while the final exothermal stage at 290.84 °C is attributed to the decomposition process of CS [4,18]. The results of FTIR spetrum and DSC obviously demonstrated the successful grafting copolymerization of CS–PEG.

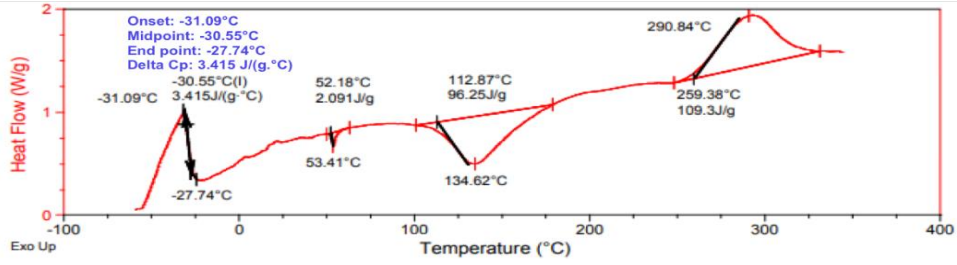

Figure 7. DSC result of CS–PEG.

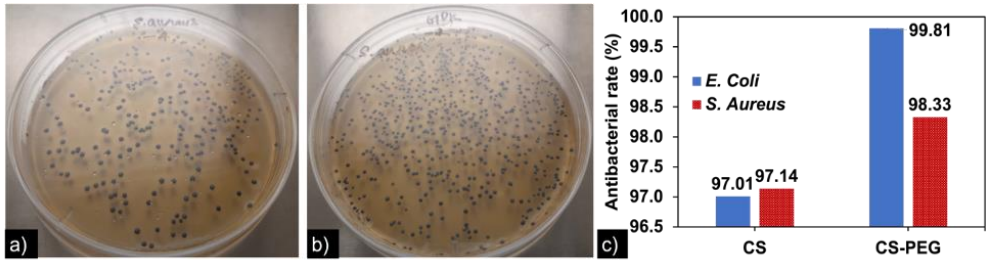

Figure 8. The antibacterial property of (a) CS, (b) CS–PEG and (c) the comparison between them.

The antibacterial activity tested with *E. coli* (as a gram-negative bacterium) and *S. aureus* (as a gram-positive bacterium) based on the Colony-count technique in the Petri dishes of CS and CS–PEG is presented in Figure 8. CS itself shows an antibacterial rate of ~ 97% for both kinds of bacteria. After grafting with PEG, the antibacterial rates for *E. coli* and *S. aureus* increase to 99.81% and 98.33%, respectively. Compared to previous reports, CS grafting poly(methyl methacrylate) with 0.72% AgNPs obtained an antibacterial rate of 95% for *E. coli* and 94% for *S. aureus* [19], both of which are much lower than those of CS–PEG without any AgNPs in this paper. CS grafting poly(*n*-butyl acrylate) with 0.22% AgNPs was also proved to against *E. coli* and *S. aureus* with the rates of 98.85% and 96.69% [4], slightly weaker than CS–PEG. This result demonstrates the high antibacterial effect of CS–PEG, which is highly potential to be applied in medical and biotechnology fields.

4. CONCLUSION

The CS–PEG grafting copolymer product was successfully synthesized via the two-stage method. The results showed that the PEG–CHO conversion reaction is significantly affected by the reaction temperature and $AgNO_3$ catalytic concentration due to the easy aggregation of the generated AgNPs, which greatly reduces the reactivity of functional groups. As a result, the temperature of 80 °C and $AgNO_3$ catalytic concentration of 0.75% can facilitate the conversion reaction with the highest efficiency of 80%. At the next stage, the grafting reaction of PEG onto CS obtains the highest grafting percentage and efficiency (90% and 35%, respectively) with the conditions: $–NH_2$/–CHO molar ratio of 10, $NaBH_4$/PEG–CHO molar ratio of 7.4 in 6 hours. The flexibility of CS was improved after grafting with PEG, which property is an enormous drawback of pristine CS, demonstrated through a drastic decrease in the glass transition temperature to – 31 °C. More importantly, the antibacterial activity of CS–PEG against *E. coli* and *S. aureus* was not decreased but slightly enhanced to ~ 99.81% and 98.33%, respectively. This research shows the potential of CS–PEG product with flexible mechanical property and high antibacterial ability to be used as an antibacterial coating in food industry sectors.

REFERENCES

1. S.R. Balusamy, S. Rahimi, J. Sukweenadhi, S. Sunderraj, R. Shanmugam, L. Thangavelu, I. Mijakovic, H. Perumalsamy - Chitosan, chitosan nanoparticles and modified chitosan biomaterials, a potential tool to combat salinity stress in plants, Carbohydr. Polym. **284** (2022) 119189-119210.
2. U. Chadha, P. Bhardwaj, S.K. Selvaraj, K. Kumari, T.S. Isaac, M. Panjwani, K. Kulkarni, R.M. Mathew, A.M. Satheesh, A. Pal, N. Gunreddy, O. Dubey, S. Singh, S. Latha, A. Chakravorty, B. Badoni, M. Banavoth, P. Sonar, M. Manoharan, V. Paramasivam - Advances in chitosan biopolymer composite materials: from

bioengineering, wastewater treatment to agricultural applications, Mater. Res. Express. **9** (2022) 1-36.

3. F. Croisier, C. Jérôme - Chitosan-based biomaterials for tissue engineering, Eur. Polym. J. **49** (2013) 780-792.
4. H. Yilmaz Atay - Antibacterial activity of chitosan-based systems, Funct. Chitosan, Springer Singapore, Singapore (2019) 457-489.
5. L.T.T. Ha, C.N. Mai - Synthesis and antibacterial activity of composite based on chitosan-grafted-(n-butyl acrylate) and silver nanoparticles, Vietnam J. Sci. Technol. **57** (2019) 309-319.
6. M. Kaliva, A. Georgopoulou, D.A. Dragatogiannis, C.A. Charitidis, M. Chatzinikolaidou, M. Vamvakaki - Biodegradable chitosan-graft-Poly(L-lactide) copolymers for bone tissue engineering, Polymers (Basel) **12** (2020) 316-335.
7. M.-Y. Wong, B. Amini Horri, B. Salamatinia - Grafted copolymerized chitosan and its applications as a green biopolymer, Biopolym. Grafting Appl., Elsevier (2018) 285-333.
8. N.M. Chau, T.T.H. La, M.T. Sam - Synthesis of chitosan-graft-polyaniline with the conductive potential, Vietnam J. Sci. Technol. **59** (2021) 12-22.
9. C. Duan, X. Meng, J. Meng, M.I.H. Khan, L. Dai, A. Khan, X. An, J. Zhang, T. Huq, Y. Ni - Chitosan as a preservative for fruits and vegetables: A review on chemistry and antimicrobial properties, J. Bioresour. Bioprod. **4** (2019) 11-21.
10. J. Wang, Y. Li, Y. Peng, G. Song - Silver nitrate-catalyzed selective air oxidation of benzylic and allylic alcohols to corresponding aldehydes or ketones, J. Chinese Chem. Soc. **61** (2014) 517-520.
11. L.T.T. Ha, C.N. Mai - Modifying chitosan with *n*-butyl acrylate - antibacterial ability, Sci. Technol. Dev. Jounal Sci. Earth Environ. **2** (2018) 12-18.
12. C. Luo, Y. Zhang, X. Zeng, Y. Zeng, Y. Wang - The role of poly(ethylene glycol) in the formation of silver nanoparticles, J. Colloid Interface Sci. **288** (2005) 444-448.
13. Q. Luo, H. Gao, L. Peng, G. Liu, Z. Zhang - Synthesis of PEGylated chitosan copolymers as efficiently antimicrobial coatings for leather, J. Appl. Polym. Sci. **133** (2016) 43465-43472.
14. Y. Monsalve, G. Tosi, B. Ruozi, D. Belletti, A. Vilella, M. Zoli, M.A. Vandelli, F. Forni, B.L. López, L. Sierra - PEG-g-chitosan nanoparticles functionalized with the monoclonal antibody OX26 for brain drug targeting, Nanomedicine **10** (11) (2015) 1735-1750.
15. Y. Dong, Y. Ruan, H. Wang, Y. Zhao, D. Bi - Studies on glass transition temperature of chitosan with four techniques, J. Appl. Polym. Sci. **93** (2004) 1553-1558.
16. P. Törmälä - Determination of glass transition temperature of poly(ethylene glycol) by spin probe technique, Eur. Polym. J. **10** (1974) 519-521.
17. M. Polaskova, P. Peer, R. Cermak, P. Ponizil - Effect of thermal treatment on crystallinity of poly(ethylene oxide) electrospun fibers, Polymers (Basel) **11** (2019) 1-9.
18. F. Ferrero, M. Periolatto - Antimicrobial finish of textiles by chitosan UV-curing, J. Nanosci. Nanotechnol. **12** (2012) 4803-4810.
19. J. An, X. Yuan, Q. Luo, D. Wang - Preparation of chitosan-graft-(methyl methacrylate)/Ag nanocomposite with antimicrobial activity, Polym. Int. **59** (2010) 62-70.

TÓM TẮT

TỔNG HỢP CHITOSAN-GHÉP-POLY(ETHYLENE GLYCOL) VỚI KHẢ NĂNG KHÁNG KHUẨN

Châu Ngọc Mai[1,2,3], La Thị Thái Hà[2,3,*],
Trần Trung Hiếu[2,3], Nguyễn Thuỳ An[2,3]
[1]*Trường Đại học Công nghiệp Thực phẩm TP.HCM*
[2]*Trường Đại học Bách Khoa TP.HCM*
[3]*Đại học Quốc gia TP.HCM*
*Email: *lathaihapolyme@hcmut.edu.vn*

Chitosan là một trong những polyme dồi dào nhất trong tự nhiên và có tiềm năng rất lớn trong nhiều lĩnh vực hiện nay nhờ vào khả năng kháng khuẩn vốn có và tính chất đặc biệt của nó như một polyme sinh học. Tuy nhiên, độ giòn cao và cơ tính thấp đã giới hạn khả năng ứng dụng của chitosan trong thực tế. Do đó, trong nghiên cứu này, poly(ethylene glycol) (PEG) được lựa chọn ghép với CS nhờ vào tính linh động cao, có thể bù đắp cho tính giòn của chitosan, và đồng thời cũng an toàn với con người. Nghiên cứu hướng đến tổng hợp chitosan ghép PEG (CS–PEG) bằng phương pháp hai giai đoạn với tỷ lệ và hiệu suất ghép cao và đánh giá tính kháng khuẩn của CS–PEG sau khi biến tính. Đầu tiên, PEG được chuyển hoá thành PEG-aldehyde để tạo thành nhóm –CHO trung gian cho phản ứng ghép với $–NH_2$ của CS. Kết quả cho thấy ở điều kiện nhiệt độ 80 °C và nồng độ $AgNO_3$ 0,75%, hiệu suất đạt được cao nhất ở 77 %. Ở giai đoạn ghép CS–PEG, tỷ lệ nhóm chức $–NH_2$/–CHO đóng vai trò quyết định mức độ ghép. Phản ứng đạt được phần trăm ghép và hiệu suất ghép cao nhất (90 và 35%) khi tỷ lệ mol nhóm chức $–NH_2$/–CHO = 10, tỷ lệ mol $NaBH_4$/PEG–CHO = 7,4 và phản ứng trong 6 giờ. CS–PEG cho thấy nhiệt độ chuyển thuỷ tinh đã giảm xuống còn – 31 °C, chứng minh sự tăng cường về độ mềm dẻo của mạch chitosan. Ngoài ra, hiệu ứng kháng khuẩn của CS–PEG đạt 99,8 và 98,3% đối với vi khuẩn *E. coli* và *S. aureus*, cho thấy tiềm năng to lớn của nó để có thể ứng dụng vào lĩnh vực thực phẩm như một lớp phủ kháng khuẩn.

Từ khoá: Polyme kháng khuẩn, chitosan ghép poly(ethylene glycol), phản ứng ghép copolyme, polyme nguồn gốc thiên nhiên.